



# OMCAT: OMNI CONTEXT AWARE TRANSFORMER

**Anonymous authors**

Paper under double-blind review

## ABSTRACT

Large Language Models (LLMs) have made significant strides in text generation and comprehension, with recent advancements extending into multimodal LLMs that integrate visual and audio inputs. However, these models continue to struggle with fine-grained, cross-modal temporal understanding, particularly when correlating events across audio and video streams. We address these challenges with two key contributions: a new dataset and model, called OCTAV and OMCAT respectively. OCTAV (**O**mn**i** **C**ontext and **T**emporal **A**udio **V**ideo) is a novel dataset designed to capture event transitions across audio and video. Second, OMCAT (**O**mn**i** **C**ontext **A**ware **T**ransformer) is a powerful model that leverages RoTE (Rotary Time Embeddings), an innovative extension of RoPE, to enhance temporal grounding and computational efficiency in time-anchored tasks. Through a robust three-stage training pipeline—feature alignment, instruction tuning, and OCTAV-specific training—OMCAT excels in cross-modal temporal understanding. Our model demonstrates state-of-the-art performance on Audio-Visual Question Answering (AVQA) tasks and the OCTAV benchmark, showcasing significant gains in temporal reasoning and cross-modal alignment, as validated through comprehensive experiments and ablation studies. Our dataset and code will be made publicly available. The link to our demo page is <https://om-cat.github.io>.

## 1 INTRODUCTION

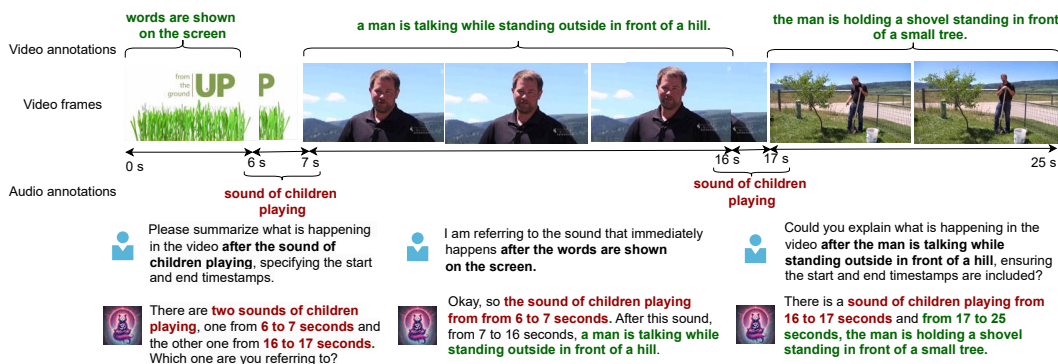


Figure 1: Illustration of a video sequence from our proposed OCTAV dataset. The annotations highlight key moments, including the timing of the audio and visual events.

Large language models (LLMs) (Achiam et al., 2023; Touvron et al., 2023) have achieved remarkable breakthroughs in both text generation and comprehension (McKeown, 1992; Achiam et al., 2023) tasks. Since then, significant progress has been made to extend LLMs to multimodal LLMs (Cheng et al., 2024; Li et al., 2023b; Maaz et al., 2023; Li et al., 2024), which integrate visual and audio inputs with textual instructions to provide understanding in multimodal contexts (Yang et al., 2022b; Chen et al., 2023a;b). These models, however, are limited in their cross-modal understanding and in their ability to provide answers to questions with fine-grained timestamps or anchored on events, as shown in Figure 1. In this paper, we address these limitations by proposing a new dataset OCTAV and

054 a model called OMCAT. The Omni Context and Temporal Audio Video dataset, OCTAV, consists of  
055 question-answer pairs for a video. Each question captures the transition between the events happening  
056 in the video through a sound event (e.g. Figure 1). The Omni Context Aware Transformer, OMCAT,  
057 addresses the limitations of existing models (Maaz et al., 2023; Tang et al., 2024; Su et al., 2023;  
058 Cheng et al., 2024) through a unified audio and visual language model by effectively incorporating  
059 time representations to ground the modalities temporally.

060 Despite the notable progress in multimodal LLMs (Li et al., 2023b; Maaz et al., 2023; Cheng et al.,  
061 2024; Lyu et al., 2023), most advancements have been centered around developing domain specific  
062 models in isolation, typically Video LLMs (Wang et al., 2023; Fu et al., 2024) or Audio LLMs (Gong  
063 et al., 2023; Kong et al., 2024; Chu et al., 2023). However, these models still face challenges in  
064 handling fine-grained, cross-modal temporal understanding when both audio and video are provided.  
065 For instance, if a user asks the question, “Is it raining in the video?” This question can be answered  
066 by either just looking at the video or listening to the audio. However, as shown in Figure 1, if the  
067 user asks the question, “Describe what happens in the video after the sound of children playing?”,  
068 the model must understand both modalities because the sound of `children playing` cannot be  
069 seen, only heard, and `what the man is doing` cannot be heard, only seen. Achieving this is  
070 challenging due to several reasons, including the lack of temporally aligned cross-modal datasets,  
071 unified models and benchmarks, and clear understanding of how to combine modalities effectively.

072 Our goal is to achieve this cross-modal temporal understanding, and to this end we propose an  
073 instruction tuning dataset called OCTAV: **O**mn**i** **C**ont**e**xt and **T**emporal **A**udio **V**ideo. Figure 1 shows  
074 a sample from our proposed OCTAV dataset. Existing audio and video understanding datasets (Chen  
075 et al., 2023b;a; 2020; Geng et al., 2023) only focus on open-ended question answering tasks (Yang  
076 et al., 2022b; Li et al., 2022) for audio-visual events. They lack the ability to temporally ground events  
077 or describe events that involve ambiguity or missing information in one of the modalities. Specifically,  
078 we create question-answer pairs for a video such that each question captures the transition between  
079 the events happening in the video through a sound event. For instance, as shown in Figure 1, we  
080 add the sound event of `children playing` to the silent input video between 6 to 7 seconds,  
081 during which nothing substantial happens in the video. Then, we capture the video event `before`  
082 `6 seconds` and `after 7 seconds` while using the sound of `children playing` as a  
083 transition event. This setting encourages the model to not only understand the relationship between  
084 the audio and the video, but also a strong temporal understanding of both the audio and video domains  
085 in a single setup. Despite this artificial setup, our experiments show that a model trained with this

086 While dataset design is necessary, it is not a sufficient condition to achieve cross-modal understanding  
087 given the challenges in modelling such data. As such, we propose a new approach that embeds abso-  
088 lute and relative temporal information in the audio and visual features, improving the model’s ability  
089 to become temporally-aware. With the goal of improving cross-modal and temporal understanding,  
090 and following common practice in multimodal LLMs (Li et al., 2023b; Cheng et al., 2024; Li et al.,  
091 2024; Tang et al., 2024; Fu et al., 2024), we divide model training into 3 stages. The first training  
092 stage is focused on feature alignment, and uses audio-text, video-text, and audio-video-text data (Liu  
093 et al., 2024; Mei et al., 2024; Chen et al., 2023b). In the second stage, the model is instruction-tuned  
094 with data (Luo et al., 2023; Li et al., 2023b; Drossos et al., 2020; Chen et al., 2020) that promotes  
095 temporal and cross-modal understanding. Finally, the model is trained to support complex and  
096 cross-modal temporal data in the OCTAV dataset as shown in Figure 1. We name the model trained  
097 with our proposed OCTAV dataset and the temporal conditioning strategy OMCAT, for **OM**ni **C**ont**e**xt  
098 **A**ware **T**ransformer. Through this learning strategy, our method outperforms existing models on  
099 AVQA tasks (Yang et al., 2022b; Li et al., 2022) and beats baselines by a significant margin on our  
100 proposed OCTAV benchmark dataset.

100 In summary, our main contributions are as follows:

- 101 - We introduce a novel method for generating synthetic instruction-tuning dataset, OCTAV, which has  
102 temporal and contextual audio and video question/answer pairs addressing the limitations of existing  
103 datasets. This dataset has both training and evaluation samples to promote research in this direction.
- 104 - We propose OMCAT: a unified, temporally-aware audio and visual language model with fine-  
105 grained and cross-modal understanding, achieved through a staged training strategy that leverages all  
106 combinations of audio, video and text data.
- 107 - We propose RoTE: a simple yet efficient modification to RoPE that provides better scores on  
benchmarks and better computational efficiency than existing approaches for temporal conditioning,

108 especially on time-anchored tasks.

109 - Finally, we exhaustively evaluate OMCAT, including ablations, on a variety of multimodal tasks. Our  
 110 experiments demonstrate that our model raises the standards on AVQA tasks, temporal understanding  
 111 tasks and our proposed OCTAV benchmark.

## 113 2 RELATED WORK

114 **Multimodal LLMs.** Since the rise of large language models (LLMs) (Achiam et al., 2023; Chiang  
 115 et al., 2023; Touvron et al., 2023), there has been growing interest in integrating additional modalities  
 116 (Cheng et al., 2024; Gong et al., 2023; Kong et al., 2024). Video LLMs (Li et al., 2023b; Fu et al.,  
 117 2024; Wang et al., 2023) utilize video-text datasets to address tasks like video question answering (Xu  
 118 et al., 2016; Yu et al., 2019), visual grounding (Kazemzadeh et al., 2014), and understanding temporal  
 119 segments (Gao et al., 2017; Huang et al., 2024). These have evolved into multimodal LLMs (Cheng  
 120 et al., 2024; Maaz et al., 2023; Lyu et al., 2023), which encode multiple modalities and focus on  
 121 coarse-grained tasks like audio-video understanding and question answering (Shu et al., 2023; Chen  
 122 et al., 2023a; Yang et al., 2022b). However, these models struggle with fine-grained audio-visual  
 123 tasks, where precise synchronization is key to deeper event comprehension.

124 Recent efforts have attempted to address this. GroundingGPT (Li et al., 2024) predicts fine-grained  
 125 timestamps but is limited to sound events, while AVicuna (Tang et al., 2024) takes a more balanced  
 126 approach to audio-visual temporal understanding. However, both models fall short in capturing  
 127 intricate cross-modal temporal dynamics. Our work aims to address these gaps by focusing on  
 128 fine-grained cross-modal information integration.

129 **Instruction tuning datasets.** GPT-based methods have been widely used to create datasets for video,  
 130 audio, and audio-visual tasks, advancing multimodal models with large-scale resources. In video  
 131 understanding, they generate and annotate datasets for tasks like video captioning (Fu et al., 2024),  
 132 video question answering (Xu et al., 2016; Yu et al., 2019), and action recognition (Yu et al., 2019).  
 133 Similarly, for audio understanding, instruction tuning datasets (Kong et al., 2024; Goel et al., 2024)  
 134 target sound events (Salamon et al., 2014), audio captioning (Kim et al., 2019), and audio question  
 135 answering (Lipping et al., 2022). Recently, AI-generated datasets have also progressed in audio-visual  
 136 tasks like captioning (Chen et al., 2023a), question answering (Yang et al., 2022b), and dialog (Alamri  
 137 et al., 2019). Despite this progress, current datasets remain predominantly coarse-grained, lacking  
 138 fine-grained temporal and cross-modal synchronization. Our proposed dataset, OCTAV, addresses  
 139 this limitation, enabling more precise alignment between audio and visual cues in complex scenarios.

## 140 3 THE OCTAV DATASET

141 One of the challenges in developing models that can understand strongly timestamped and anchored  
 142 events is the lack of datasets that have this information (Wang et al., 2023; Liu et al., 2024; Chen  
 143 et al., 2020; Li et al., 2023b; Tang et al., 2024; Lyu et al., 2023). To overcome this limitation, we  
 144 propose a pipeline to generate a synthetic dataset called OCTAV, for **O**mn **C**ontext **T**emporal **A**udio  
 145 **V**ideo dataset. Figure 1 shows an example from our proposed OCTAV dataset. First, we discuss how  
 146 we identify relevant event transitions in videos. Then, we discuss how we anchor those transitions on  
 147 audio samples and finally, we show how to generate question-answer pairs for these synthetically  
 148 curated videos.

149 **Identifying transitions between video events.** To achieve this, we utilize videos with strongly  
 150 timestamped captions (Zhou et al., 2018; Krishna et al., 2017; Tang et al., 2019; Zala et al., 2023),  
 151 *i.e.* a video  $V$  with time-caption pairs  $\{(t_1, c_1), (t_2, c_2) \dots (t_k, c_k)\}$ , where  $k$  is the total number of  
 152 time chunks annotated in the video. Given a list of timestamped video captions indexed by  $i$  and  
 153 bounded by start time ( $t_i^s$ ) and end time ( $t_i^e$ ) each, we find pairs where the gap between end time and  
 154 start time is smallest than  $m$  and the sum of their lengths, from earliest to latest, is at most  $T$  seconds.  
 155 Empirically we set  $m = 10$  and  $T = 30$ , ensuring that the videos are not too far apart and their length  
 156 is not too long. Next, we discuss how to anchor sound between these video event transitions.

157 **Anchoring chunked videos on a single sound event.** For these chunked videos, we inject a sound  
 158 event between the timestamp  $t_i^e$  and  $t_j^s$ . More specifically, we randomly sample a sound event  $s$  from  
 159 a variety of different sound sources (Salamon et al., 2014; Fonseca et al., 2021; Piczak, 2015; Rashid  
 160 et al., 2023). Details of these sound sources are provided in Appendix C.4. We remove the original  
 161 audio in the given video chunk and insert this sound event between the timestamp  $\{t_i^e, t_j^s\}$  to create a

strongly timed video chunk anchored on a sound event. We refer to this subset of the dataset as the OCTAV-ST dataset where, ST is for single-turn.

**Anchoring chunked videos on multiple sound events.** We extend the videos from a single sound event to two sound events as shown in Figure 1. Particularly, we first create a chunked video with three unique events  $c_i, c_j,$  and  $c_k$  corresponding to timestamps  $t_i, t_j$  and  $t_k$  respectively, following the same procedure discussed previously. Then, we add a random sound event after removing the original audio between the timestamps  $\{t_i^e, t_j^s\}$  and  $\{t_j^e, t_k^s\}$ . We refer to this subset with interwoven and timestamped videos with audio events as the OCTAV-MT dataset where, MT stands for multi-turn.

**Creating question-answer pairs.** Here, we discuss how to create question-answer pairs for the interwoven videos in the OCTAV-ST and OCTAV-MT dataset. Essentially, we have two (or three) video caption events for each chunked video and an associated audio event/sound between the video events. The model has to generate questions such that it can capture *what event is happening in the video {before the sound event, after the sound event}*, and *clarify which of the sound events the user is referring to while answering the question*. We use GPT-assisted (Achiam et al., 2023) generation to generate a diverse set of question-answer pairs. The prompts used are given in Appendix C.1 and Appendix C.2 and the list of instructions are given in the Appendix C.3.

Table 1: Statistics with number of videos and question-answer pairs for the OCTAV-ST dataset.

OCTAV-ST	Train	Test
	#Videos (QA Pairs)	#Videos(QA Pairs)
Youcook2 (Zhou et al., 2018)	6832	2414
ActivityNet (Krishna et al., 2017)	16072	6228
QueryD (Onescu et al., 2021)	16985	-
COIN (Tang et al., 2019)	31938	-
HiREST (Zala et al., 2023)	2408	-
Total	127,507	8642

Table 2: Statistics with number of videos and question-answer pairs for the OCTAV-MT dataset.

OCTAV-MT	Train	Test
	#Videos, #QA Pairs	# Videos, #QA Pairs
Youcook2 (Zhou et al., 2018)	4296, 34330	1476, 11806
ActivityNet Krishna et al. (2017)	6463, 51670	1362, 10858
UnAV-100-MT	14698, 94916	2043, 9694
Total	25,457, 180,916	4,881, 32,358

**Dataset Statistics.** We utilize timestamped videos from Youcook2 (Zhou et al., 2018), QueryD (Onescu et al., 2021), ActivityNet (Krishna et al., 2017), COIN (Tang et al., 2019), UnAV-100 (Geng et al., 2023) and, HiREST (Zala et al., 2023) datasets to create chunked videos. Essentially, we use these datasets as they have segmented annotations available for videos in diverse domains such as cooking, daily activities, scenes and instructional videos.

Overall, the OCTAV-ST dataset has 127,507 unique videos with single question-answer pairs for each video for training. For evaluation, we provide 2414 unique videos with question-answer pairs from the test subset of Youcook2 (Zhou et al., 2018), denoted as OCTAV-ST-Youcook2 and 6228 unique videos with question-answer pairs from the test subset of the ActivityNet dataset (Krishna et al., 2017), called as OCTAV-ST-ActivityNet. In Table 1, we show the breakdown of our proposed OCTAV-ST dataset in detail.

The OCTAV-MT dataset has 25,457 unique videos/multi-turn dialogues with a total of 180,916 single question-answer pairs for training. In Table 2, we show the detailed statistics of our proposed OCTAV-MT dataset. Specifically, we curate synthetic chunked videos for Youcook2 and ActivityNet and use the original videos from UnAV-100 dataset (Geng et al., 2023). The UnAV-100 dataset has timestamped audio-visual annotations from videos with real-time audio events and we convert this into question-answer pairs called the OCTAV-MT dataset (e.g. shown in Figure 7). We train and evaluate on this dataset to show OMCA’s performance on in-the-wild and naturally occurring audio-visual settings. For evaluation on this multi-turn setup, we provide a total of 4818 unique videos with 32,358 question-answer pairs. Example annotations from both the OCTAV-ST and OCTAV-MT are given in Appendix D.

Table 3: Comparison of our proposed OCTAV dataset with other datasets with respect to modalities (audio/video), caption availability, multi-turn setup and timestamp information.

Dataset	Audio	Video	Detailed captions	Multi-turn	Timestamps
InternVid (Wang et al., 2023)	✓	✓	✓	✓	✓
VALOR (Chen et al., 2023a)	✓	✓	✓	✗	✓
VAST (Chen et al., 2023b)	✓	✓	✓	✗	✗
VGG-Sound (Chen et al., 2020)	✓	✓	✗	✗	✗
UnAV-100 (Geng et al., 2023)	✓	✓	✗	✗	✓
OCTAV	✓	✓	✓	✓	✓

**Comparison to existing datasets** In Table 3, we compare our proposed OCTAV dataset to existing datasets in the audio and video domains. Most of these datasets are limited to either the video

modality (Wang et al., 2023), have missing timestamp information (Chen et al., 2023a;b; 2020), do not offer multi-turn question-answer pairs (Chen et al., 2023a;b; 2020; Geng et al., 2023) or have single event classes rather than detailed captions (Chen et al., 2020; Geng et al., 2023). OCTAV dataset addresses all the above mentioned limitations and provides a comprehensive benchmark for interwoven and fine-grained audio-visual understanding.

## 4 THE OMCAT APPROACH

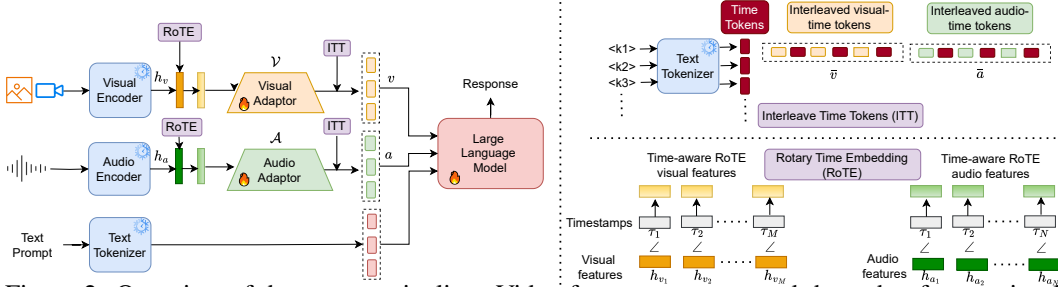


Figure 2: Overview of the OMCAT pipeline. Video frames are processed through a frozen visual encoder, while audio frames are encoded using a frozen audio encoder. Extracted features are fine-tuned through adaptor layers across all three stages. The LLM remains frozen in Stage 1 and is fine-tuned in Stages 2 and 3. The purple blocks represent time alignment modules, with only one of them activated during training.  $\angle$  in bottom right denotes the rotation angle.

In this section, we describe our proposed OMCAT model, depicted in Figure 2. We begin by discussing the model architecture and feature extraction in Section 4.1, followed by time alignment between audio and video in Section 4.2. Next, we discuss the prompt design to query the LLM in Section 4.3 and finally, we detail the multi-stage training process of OMCAT in Section 4.4.

### 4.1 MODEL ARCHITECTURE AND FEATURE EXTRACTION

**Multi-modal Feature Extraction.** As shown in Figure 2, OMCAT uses a visual encoder,  $f_v(\cdot)$  and an audio encoder,  $f_a(\cdot)$ . Given a video  $V$  and an audio  $A$ , the encoded hidden features for the two modalities are represented as:

$$h_v = f_v(V), \quad h_a = f_a(A) \quad (1)$$

where  $h_v \in \mathbb{R}^{M \times d_v}$  are the extracted features for the video modality with  $M$  frames extracted uniformly from the video and  $d_v$  as the hidden dimension.  $M$  is 1 if the modality is image. The features for the audio modality are denoted as  $h_a \in \mathbb{R}^{N \times d_a}$ , where  $N$  are the time windows for which the audio features are computed and  $d_a$  is the hidden dimension.

**Audio-Visual Adaptors.** To map the video modality and audio modality to the text embedding space of the LLM (Chiang et al., 2023), we use two adaptor blocks: one for the video modality denoted as  $\mathcal{V}(\cdot)$  and another for the audio modality denoted as  $\mathcal{A}(\cdot)$ . Essentially, the encoded hidden features are passed to the adaptors to extract token embeddings as:

$$v = \mathcal{V}(h_v), \quad a = \mathcal{A}(h_a) \quad (2)$$

These tokens are then used as prompts to the LLM along with the time representations. Following prior work (Cheng et al., 2024; Li et al., 2024), we use the fine-tuned vicuna 7B-v1.5 (Chiang et al., 2023) as our LLM to generate the final text responses. Next, we discuss how to incorporate time into our model.

### 4.2 TIME ALIGNMENT BETWEEN AUDIO AND VIDEO

Existing multimodal LLMs rely on learnable positional embeddings to encode the order of frames, but they struggle to capture the absolute time elapsed between frames and lack a fine-grained, cross-modal understanding of audio and video. We propose two strategies to encode absolute and relative temporal information on video and audio tokens, called Interleaving Time Tokens (ITT) and Rotary Time Embeddings (RoTE).

**Interleaving Time Tokens (ITT).** In this approach, we interleave time tokens with the audio and the visual features. We allocate a budget of  $K$  learnable time tokens, zero-indexed by  $k_i$ , and assign a time token to an audio-visual feature with the following indexing function:

$$k_i = \text{round} \left( \frac{\tau_i}{T} \cdot (K - 1) \right) \quad (3)$$

where  $\tau_i$  is a continuous timestamp in seconds,  $T$  is the total duration of the video or audio in seconds, and  $K$  is the total number of learnable time tokens.

For a video  $V$  with duration  $T$  and video token embeddings  $v_i$  where  $i = 1 \dots M$ , each embedding is associated with a timestamp  $\tau_i$  (e.g. 0.5 seconds, 1.4 seconds, and so forth). We first use these timestamps to obtain the discrete time tokens, then we interleave them with the visual tokens  $v_i$  obtained after the visual adaptor layers. Specifically, each visual token  $v_i$  corresponds to a discrete time token indexed by  $k_i$ , as described in Equation (3). Hence, the interleaved visual sequence is given as  $\bar{v} = \{v_1, \langle k_1 \rangle, v_2, \langle k_2 \rangle \dots, \langle v_M \rangle, \langle k_M \rangle\}$ .

Similarly, for the given audio  $A$  of duration  $T$ , we extract  $N$  windows of length  $w$  from the audio sequence such that for each window the time is represented as:  $\tau_n = [n, n + w]$  for  $n = 1, 2, \dots, N$ , where  $n$  is the time in seconds. We then take the mean of the time windows,  $\tau_n = \frac{n+(n+w)}{2}$ . Then, we convert  $\tau_n$  into discrete time token  $k_n$  using Equation (3) and interleave them with the audio tokens  $a$  obtained from the audio adaptor layers. Hence, the interleaved audio sequence is represented as  $\bar{a} = \{a_1, \langle k_1 \rangle, a_2, \langle k_2 \rangle \dots, \langle a_N \rangle, \langle k_N \rangle\}$ . The final interleaved tokens  $\bar{v}$  and  $\bar{a}$  are then concatenated with the text instructions as prompts to the LLM, as shown in Figure 2 on upper top right.

**Rotary Time Embeddings (RoTE).** While we could use RoPE (Su et al., 2024) and avoid the extra context length cost introduced by ITT, RoPE would still lack the ability to capture the absolute time elapsed between frames, which is very important and crucial in scenarios with varying frame rates. To address these limitations, we propose an alternative strategy called RoTE: a modified version of RoPE, where the rotation angles are determined by absolute timestamps in seconds instead of frame indices. RoTE takes inspiration from a real clock, where each handle rotates at distinct speeds, or “frequencies”. Similarly, in RoTE we rotate different dimensions in the visual and audio feature embeddings given their timestamp in seconds and the respective “frequency” of that dimension. Our results in Section 5 show that RoTE achieves performance that is superior to the baselines. A visual representation of RoTE is shown in Figure 1 on the lower right bottom.

In practice, while in rope the angle for rotation  $\theta$  is defined by the temporal indexing of a token  $\theta \leftarrow -i \times 2\pi$ , RoTE is defined by the absolute time  $\theta \leftarrow -\tau_i \times 2\pi$ . These temporally enriched features are then passed to the adaptor layers  $\mathcal{V}(\cdot)$  and  $\mathcal{A}(\cdot)$  to create visual tokens  $v$  and audio tokens  $a$  respectively.

### 4.3 INSTRUCTION PROMPTS

In this section, we explain how video and audio tokens are combined with text prompts. The prompt format is as follows:

User:  $\langle \text{system prompt} \rangle$  Question  $\langle vi\_start \rangle \langle vi\_patch \rangle \langle vi\_end \rangle \langle so\_start \rangle \langle so\_patch \rangle \langle so\_end \rangle \langle vis\_start \rangle \langle vi\_patch \rangle \langle so\_patch \rangle \langle vis\_end \rangle$  Assistant:

Here,  $\langle \text{system prompt} \rangle$  represents a guiding system message, following Vicuna-7B (Chiang et al., 2023). Visual and audio markers are included through tokens like  $\langle vi\_start \rangle / \langle vi\_end \rangle$  for video and  $\langle so\_start \rangle / \langle so\_end \rangle$  for audio. Video tokens ( $\langle vi\_patch \rangle$ ) encode visual information, and audio tokens ( $\langle so\_patch \rangle$ ) handle sound data. It is important to note that these individual video and audio markers are activated only when modality-specific data (video or audio) is present. For joint audio-video data,  $\langle vis\_start \rangle / \langle vis\_end \rangle$  marks the boundaries, encoding both audio and video tokens, deactivating the individual representations.

### 4.4 TRAINING STRATEGY

**Stage I: Alignment Tuning Stage.** In this stage, we train the visual and audio adaptor layers and freeze the parameters of the pre-trained visual and audio encoders as well as the LLM, as shown in Figure 2. By doing so, the model can focus on learning robust features for the adaptor layers,

Table 4: List of datasets used for training OMCAT. TS indicates if timestamps are available. ST refers to single-turn question answers. MT is the version with multi-turn dialogue.

Stage	Modality	Datasets	TS	#(Modality, Text)
Stage I Alignment Tuning	Image	LLaVA-Pretrain-595k (Liu et al., 2024)	✗	558128
	Audio	WavCaps (Mei et al., 2024)	✗	403044
	Video	Valley-703K (Luo et al., 2023)	✗	703000
	Video	VATEX (Wang et al., 2019)	✗	227250
	Audio-Video	VAST (Chen et al., 2023b)	✗	414602
	Audio-Video	VALOR (Chen et al., 2023a)	✗	16109
Stage II Instruction Tuning	Image	LLaVA-Tune (Liu et al., 2024)	✗	624610
	Audio	VGG Sound (Chen et al., 2020)	✗	5157
		AudioCaps (Kim et al., 2019)	✗	49838
		MusicCaps (Agostinelli et al., 2023)	✗	2858
		Clotho (Drossos et al., 2020)	✗	3938
		AudioSet-Strong (Hershey et al., 2021)	✓	431131
		VideoInstruct 100K (Maaz et al., 2023)	✗	98145
	VideoChatGPT (Maaz et al., 2023)	✗	100010	
	WebVidQA (Yang et al., 2022a)	✗	100000	
	Valley-Instruct 65k (Luo et al., 2023)	✗	64690	
	VideoChat-Instruct (Li et al., 2023b)	✗	6961	
	Activitynet captions (Krishna et al., 2017)	✗	7481	
	NextQA (Xiao et al., 2021)	✗	34132	
	DiDeMO (Anne Hendricks et al., 2017)	✓	27935	
	Charades (Gao et al., 2017)	✓	12408	
	ActivityNet-RTL (Huang et al., 2024)	✓	33557	
	Youcook2 (Zhou et al., 2018)	✓	8643	
	ActivityNet Dense captions (Krishna et al., 2017)	✓	33212	
	Audio-Video	Macaw Instruct (Lyu et al., 2023)	✗	50656
		AVQA (Yang et al., 2022b)	✗	40425
Music-AVQA (Li et al., 2022)		✗	25854	
UnAV-100 (Geng et al., 2023)		✓	10358	
OCTAV-ST (Ours)		✓	127507	
Stage III Multi-turn Instruction Tuning		Audio-Video	AVSD (Alamri et al., 2019)	✗
		UnAV-100-MT (Ours)	✓	94916
		OCTAV-MT (Ours)	✓	86000

which play a key role in bridging the gap between the raw audio-visual inputs and the semantic representations of the LLM.

Table 4 lists the image-text pairs (Liu et al., 2024), video-text pairs (Luo et al., 2023; Wang et al., 2019), and audio-text pairs (Mei et al., 2024) that were used to train the visual and audio adaptor layers such that the visual and audio representations are “aligned” with their corresponding textual description. In addition to these individual modalities, we also incorporate joint audio-video-text paired data (Chen et al., 2023b;a) to simultaneously train both the audio and visual adaptor layers. In total, we approximately use  $\sim 2.3M$  training data. This joint training process helps the model develop a deeper understanding of the relationships between the audio and visual modalities, improving the model’s ability to handle multimodal data.

**Stage II: Instruction Tuning Stage.** Following the “alignment” of modality features in Stage I, we proceed to train OMCAT using a diverse and high-quality collection of multimodal data ( $\sim 2.8M$ ). This includes image-text, video-text, audio-text, and audio-video-text datasets that are carefully curated to prepare the model for a wide range of tasks involving video and audio. These tasks include fine-grained timestamped comprehension as well as cross-modal understanding, enabling the model to perform effectively across multiple input types. A comprehensive overview of the datasets used in this training phase is provided in Table 4. During this training stage, we freeze the parameters of both the visual and audio encoders. We only fine-tune the visual and audio adaptor layers, along with the large language model (LLM), allowing these components to be further optimized to handle multimodal tasks.

**Stage III: Multi-Turn Instruction Tuning Stage.** In the third and final stage, our main focus is to enhance the capabilities of OMCAT on multi-turn question answering in complex audio-visual scenarios. To achieve this, we fine-tune our model on multi-turn datasets, including our proposed OCTAV-MT, UnAV-100-MT, and AVSD (Alamri et al., 2019), a dataset for audio-visual dialog. Detailed statistics of these datasets are shown in Table 4. Overall, we use  $\sim 340k$  training data during this stage. In this stage as well, the video encoder and the audio encoder remain frozen while we optimize the audio/video adaptor layers, along with the LLM.

## 5 EXPERIMENTS

**Datasets.** To evaluate the capabilities of OMCAT on general multimodal understanding, we evaluate our method on audio-visual understanding benchmarks. Specifically, we evaluate on the AVSD dataset (Alamri et al., 2019) which is a dataset for audio-visual scene aware dialog, Music-AVQA dataset (Li et al., 2022) that has audio-visual question answering for the music domain and AVQA dataset (Yang et al., 2022b) which has general questions about audio and visual modalities.

Furthermore, to evaluate whether OMCAT outperforms in temporal tasks, we measure the performance of our model on temporal video grounding benchmark, Charades-STA (Gao et al., 2017). This dataset is widely used in prior works (Cheng et al., 2024; Li et al., 2024; Ren et al., 2024) as a benchmark for temporal understanding.

Finally, we benchmark OMCAT on the evaluation subset of OCTAV-ST, OCTAV-MT and UnAV-100-MT datasets. These tasks require fine-grained temporal understanding, cross-correlation between the audio and visual modalities and hence are a good measure to evaluate the capabilities of OMCAT.

**Evaluation metrics.** Following prior work (Cheng et al., 2024; Li et al., 2024; Tang et al., 2024), we use GPT-4 (Achiam et al., 2023) to evaluate the answers predicted by the model by comparing against the correct answers, with a score of 0 to 5 indicating the accuracy. Besides Charades-STA where we use Recall@1 at Intersection over Union (IoU) thresholds of 0.5 and 0.7, we use the GPT accuracy everywhere else.

**Architecture.** We use the pre-trained CLIP visual encoder ViT-L/14 (Radford et al., 2021) to extract video/image features. For the audio encoder, we use the pre-trained ImageBind (Girdhar et al., 2023) model. Similar to previous work, for the video and audio adaptors, we use the Q-former which has the same architecture as the Q-Former in BLIP-2 (Li et al., 2023a). However, to maintain the temporal consistency of video and audio frames in the ITT setup, we replace the Q-Former adaptor layers with 2-layer transformer blocks with self-attention (Vaswani, 2017). During both training and inference, we sample 64 frames from the video and we extract five 3-second windows for the audio. The audio is resampled to 16KHz sampling rate and converted into spectrograms to be consistent with the input to the ImageBind model (Girdhar et al., 2023). We use 100 as the value of  $K$ , the learnable time tokens in Section 4.2.

**Training details.** During both the pre-training and fine-tuning stages, we train the model for one epoch on 8 NVIDIA A-100 GPUs. For the pre-training stage, we set the batch size of 64, learning rate of 1e-3 with a cosine learning decay and a warm-up period. In the fine-tuning stages, we set the batch size to 32, learning rate to 2e-5 with a cosine learning decay and a warm-up period and gradient accumulation to 2. Further details about training are given in Appendix E.

Table 5: Evaluation results for OMCAT and other state-of-the-art models on AVQA tasks (Yang et al., 2022b; Alamri et al., 2019; Li et al., 2022), Charades-STA (Gao et al., 2017) and our proposed OCTAV-ST dataset. While † describes results from models fine-tuned on the training set of those datasets, results in parentheses are zero-shot.

Method	Time	Accuracy			R@1(IoU=0.5)	R@1(IoU=0.7)	Accuracy	
		AVSD	Music-AVQA	AVQA			Charades-STA	OCTAV-ST Youcook2
PandaGPT (Su et al., 2023)	✗	26.1 <sup>†</sup>	33.7	79.8 <sup>†</sup>	-	-	-	-
Video LLaMA (Cheng et al., 2024)	✗	36.7 <sup>†</sup>	36.6	81.0 <sup>†</sup>	3.8	0.9	-	-
MacawLLM (Lyu et al., 2023)	✗	34.3 <sup>†</sup>	31.8	78.7 <sup>†</sup>	-	-	-	-
AVLLM (Shu et al., 2023)	✗	52.6 <sup>†</sup>	45.2	-	-	-	-	-
AVicuna (Tang et al., 2024)	✓	53.1 <sup>†</sup>	49.6	-	-	-	-	-
Video LLaMA 2 (Zhang et al., 2023)	✗	53.3 <sup>†</sup>	73.6 <sup>†</sup>	-	-	-	9.14	10.55
GroundingGPT (Li et al., 2024)	✓	-	-	-	29.6 <sup>†</sup>	11.9 <sup>†</sup>	1.20 <sup>†</sup> (3.87)	1.57 <sup>†</sup> (7.6)
OMCAT (RoTE)	✓	49.4 <sup>†</sup>	73.8 <sup>†</sup> (51.2)	90.2 <sup>†</sup>	32.3 <sup>†</sup>	15.9 <sup>†</sup>	16.9 <sup>†</sup> (9.9)	19.0 <sup>†</sup> (11.2)

### 5.1 QUANTITATIVE RESULTS

**Comparison to state-of-the-art.** We follow previous work (Cheng et al., 2024; Zhang et al., 2023; Shu et al., 2023) to evaluate OMCAT on three audio-video understanding benchmarks. Based on the GPT-assisted evaluation scores in Table 5, our model surpasses the most recent and relevant models on all benchmarks. While on Music-AVQA we achieve 51.2% accuracy in the zero-shot setting and 73.8% in the fine-tuned setting, outperforming SOTA models, on AVQA dataset we significantly outperform other models. We believe our competitive but relatively lower scores on AVSD comes from a difference in data distribution during the final training stage.



To evaluate temporal understanding in videos, we evaluate OMCAT Charades-STA, an established benchmark for this task. We outperform GroundingGPT (Li et al., 2024) on Recall@1 at IoU threshold of 0.5 and 0.7. This result shows that our method can also perform temporal understanding in the video domain.

Finally, we present results on the single-turn version of our proposed OCTAV benchmark, OCTAV-ST. We evaluated VideoLLaMA2 (Zhang et al., 2023) in a zero-shot setting on this dataset and fine-tuned GroundingGPT (Li et al., 2024) on the OCTAV-ST training set for a fair comparison. As shown in Table 5, our method outperforms all the above two methods in both the zero-shot (results in parantheses) and fine-tuned settings. These results confirm OMCAT’s ability to jointly learn cross-modal and temporal understanding from both video and audio data.

Table 6: Results of different variations of OMCAT (RoPE, ITT and RoTE) on the OCTAV-MT benchmark and the UnAV-100-MT dataset.

Method	Accuracy		
	OCTAV-MT-Youcook2	OCTAV-MT-ActivityNet	UnAV-100-MT
GroundingGPT (Li et al., 2024)	0.13	0.07	13.2
OMCAT (RoPE)	3.3	2.4	15.7
OMCAT (ITT)	3.1	4.1	16.6
OMCAT (RoTE)	<b>3.7</b>	<b>5.6</b>	<b>19.9</b>

**Comparison on the OCTAV-MT benchmark.** In Table 6, we highlight the performance of OMCAT on the OCTAV-MT benchmark, which involves multi-turn question-answer pairs for videos with multiple sound events. All models in Table 6 are fine-tuned on the proposed OCTAV-MT benchmark. Our model, OMCAT with RoTE, significantly outperforms the baselines—ITT, RoPE, and GroundingGPT (Li et al., 2024)—on this dataset. Moreover, it achieves substantial performance gains on the UnAV-100-MT dataset, a dataset with in-the-wild/natural audio-visual events (*e.g.* Figure 7).

OMCAT with RoTE efficiently integrates time representations with minimal computational cost, ensuring precise cross-modal alignment between audio and video. While these improvements over the baselines are considerable, there is still ample room for further enhancement in this area. The OCTAV-MT benchmark paves the way for the development of advanced multimodal models with stronger cross-modal grounding capabilities.

Table 7: Effect of applying various time embeddings—RoPE, ITT and RoTE to OMCAT on all benchmarks.

Time Encoding	Accuracy			R@1(IoU=0.5)		R@1(IoU=0.7)		Accuracy	
	AVSD	Music-AVQA	AVQA	Charades-STA		OCTAV-ST-Youcook2	OCTAV-ST-ActivityNet		
RoPE	45.9	71.2	88.2	30.7	16.1	13.3	16.5		
ITT	47.3	69.7	82.1	<b>32.5</b>	<b>16.7</b>	16.5	<b>19.2</b>		
RoTE	<b>49.4</b>	<b>73.8</b>	<b>90.2</b>	32.3	15.9	<b>16.9</b>	19.0		

Table 8: Effect of alignment tuning data on the overall performance. LP denotes LLaVA-Pretrain-595k (Liu et al., 2024), WC denotes WavCaps (Mei et al., 2024) and, V denotes Valley-703K (Luo et al., 2023).

Ablation	Music-AVQA	Charades-STA (R@1,IoU-0.5)	OCTAV-ST-Youcook2
OMCAT w/ only LP,WC,V	50.6	26.9	4.97
Ours	<b>51.2</b>	<b>32.3</b>	<b>16.9</b>

## 5.2 ABLATION STUDY

**How does time embedding affect OMCAT?** In Table 7, we evaluate three different time embedding approaches, including RoPE (Su et al., 2024), and our proposed approaches ITT and RoTE. On the AVQA benchmark, RoTE consistently outperforms the baselines by a large margin, demonstrating its strong capability not only on temporal and cross-modal tasks but also in handling coarse-grained question answering.

For the temporal understanding task on Charades-STA, ITT performs slightly better than RoTE at both IoU thresholds (0.5 and 0.7). On the OCTAV-ST benchmark, YouCook2 and ActivityNet, ITT and RoTE show nearly equivalent performance. We believe ITT’s competitive results stem from its

explicit time embedding through time tokens. However, given ITT’s increased context length and its weaker performance on AVQA tasks,  $\text{RoTE}$  is the more effective and efficient choice overall.

**What is the effect of pre-training data on OMCAT?** Furthermore, we investigate the impact of pre-training data on the final model performance, particularly during the alignment tuning stage (Stage I). This stage is crucial for establishing the model’s capacity to “align” information across different modalities, such as image, video, and audio, with text. To examine the role of joint multimodal data, we conduct an ablation study where we modify the training data by excluding the audio-video-text paired data (Chen et al., 2023b;a) while retaining image-text (Liu et al., 2024), video-text (Luo et al., 2023; Wang et al., 2019), and audio-text pairs (Mei et al., 2024).

Our results in Table 8 indicate a noticeable decline in performance across all tasks when the model is trained without audio-video-text data. This demonstrates the critical importance of joint multimodal data in achieving robust cross-modal alignment. We hypothesize that without data that directly links audio, video, and text, the model struggles to accurately capture the intricate relationships between these modalities, leading to suboptimal performance in tasks requiring fine-grained multimodal understanding.

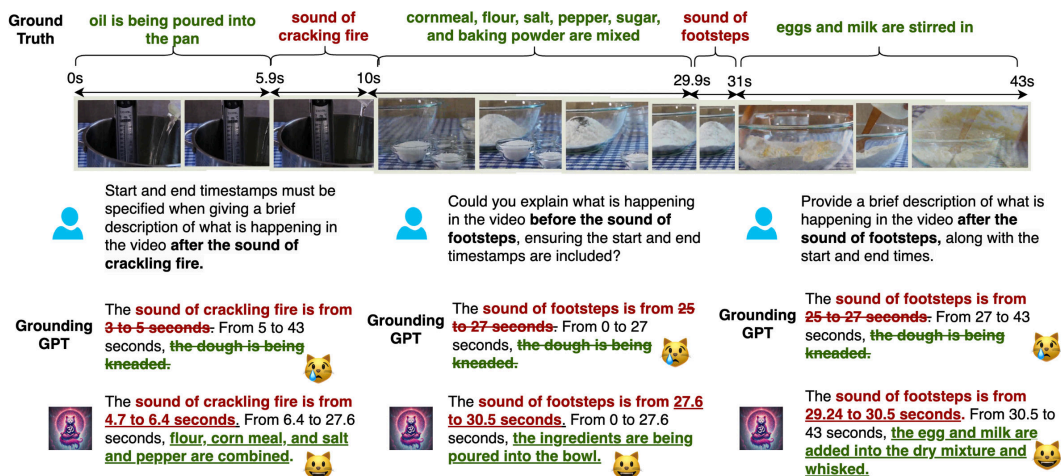


Figure 3: Qualitative comparison of OMCAT with GroundingGPT on the OCTAV-MT dataset.

### 5.3 QUALITATIVE RESULTS

In Figure 3, we showcase the qualitative performance of our method on the YouCook2 subset of the OCTAV-MT benchmark. GroundingGPT inaccurately predicts a uniform activity of *dough being kneaded*, failing to capture the nuanced transitions in events triggered by sound cues. In contrast, our model successfully isolates specific events and accurately associates them with their corresponding timestamps based on the sound events. For instance, our model correctly identifies the activity following the *sound of crackling fire* (around 6.4 to 27.6 seconds), predicting that *flour, cornmeal, and salt and pepper are combined*. This aligns closely with the ground truth, which describes the activity as *cornmeal, flour, salt, pepper, sugar, and baking powder being mixed*. While OMCAT omits some ingredients, it still recognizes the correct activity—unlike GroundingGPT, which mistakenly predicts *dough being kneaded*.

Similarly, OMCAT accurately predicts that *egg and milk are added into the dry mixture and whisked* following the *sound of footsteps* (from 29.2 to 30.5 seconds). However, when asked what occurs before the sound of footsteps, the model correctly predicts the activity as *ingredients being mixed in the bowl*, though the prediction does not perfectly match the ground truth.

## 6 CONCLUSION

In this paper, we addressed the limitations of multimodal large language models in fine-grained, cross-modal temporal understanding by introducing the OCTAV dataset and the OMCAT model. OCTAV focuses on event transitions across audio and video, promoting deeper temporal alignment and cross-modal understanding. OMCAT, enhanced with  $\text{RoTE}$  embeddings, effectively grounds temporal information across modalities, leading to superior performance on Audio-Visual Question Answering (AVQA) tasks and the OCTAV benchmark. Our approach sets a new standard for multimodal AI, advancing cross-modal and temporal reasoning capabilities for future research.

## REFERENCES

- 540  
541  
542 Josh Achiam, Steven Adler, Sandhini Agarwal, Lama Ahmad, Ilge Akkaya, Florencia Leoni Aleman,  
543 Diogo Almeida, Janko Altenschmidt, Sam Altman, Shyamal Anadkat, et al. Gpt-4 technical report.  
544 *arXiv preprint arXiv:2303.08774*, 2023.
- 545  
546 Andrea Agostinelli, Timo I Denk, Zalán Borsos, Jesse Engel, Mauro Verzetti, Antoine Caillon,  
547 Qingqing Huang, Aren Jansen, Adam Roberts, Marco Tagliasacchi, et al. Musiclm: Generating  
548 music from text. *arXiv preprint arXiv:2301.11325*, 2023.
- 549  
550 Huda Alamri, Vincent Cartillier, Abhishek Das, Jue Wang, Anoop Cherian, Irfan Essa, Dhruv Batra,  
551 Tim K Marks, Chiori Hori, Peter Anderson, et al. Audio visual scene-aware dialog. In *Proceedings  
552 of the IEEE/CVF Conference on Computer Vision and Pattern Recognition*, pp. 7558–7567, 2019.
- 553  
554 Lisa Anne Hendricks, Oliver Wang, Eli Shechtman, Josef Sivic, Trevor Darrell, and Bryan Russell.  
555 Localizing moments in video with natural language. In *Proceedings of the IEEE international  
556 conference on computer vision*, pp. 5803–5812, 2017.
- 557  
558 David Chen and William B Dolan. Collecting highly parallel data for paraphrase evaluation. In  
559 *Proceedings of the 49th annual meeting of the association for computational linguistics: human  
560 language technologies*, pp. 190–200, 2011.
- 561  
562 Honglie Chen, Weidi Xie, Andrea Vedaldi, and Andrew Zisserman. Vggsound: A large-scale audio-  
563 visual dataset. In *ICASSP 2020-2020 IEEE International Conference on Acoustics, Speech and  
564 Signal Processing (ICASSP)*, pp. 721–725. IEEE, 2020.
- 565  
566 Sihan Chen, Xingjian He, Longteng Guo, Xinxin Zhu, Weining Wang, Jinhui Tang, and Jing Liu.  
567 Valor: Vision-audio-language omni-perception pretraining model and dataset. *arXiv preprint  
568 arXiv:2304.08345*, 2023a.
- 569  
570 Sihan Chen, Handong Li, Qunbo Wang, Zijia Zhao, Mingzhen Sun, Xinxin Zhu, and Jing Liu. Vast:  
571 A vision-audio-subtitle-text omni-modality foundation model and dataset. *Advances in Neural  
572 Information Processing Systems*, 36:72842–72866, 2023b.
- 573  
574 Zesen Cheng, Sicong Leng, Hang Zhang, Yifei Xin, Xin Li, Guanzheng Chen, Yongxin Zhu, Wenqi  
575 Zhang, Ziyang Luo, Deli Zhao, et al. Videollama 2: Advancing spatial-temporal modeling and  
576 audio understanding in video-llms. *arXiv preprint arXiv:2406.07476*, 2024.
- 577  
578 Wei-Lin Chiang, Zhuohan Li, Zi Lin, Ying Sheng, Zhanghao Wu, Hao Zhang, Lianmin Zheng, Siyuan  
579 Zhuang, Yonghao Zhuang, Joseph E Gonzalez, et al. Vicuna: An open-source chatbot impressing  
580 gpt-4 with 90%\* chatgpt quality, march 2023. URL <https://lmsys.org/blog/2023-03-30-vicuna>, 3  
581 (5), 2023.
- 582  
583 Yunfei Chu, Jin Xu, Xiaohuan Zhou, Qian Yang, Shiliang Zhang, Zhijie Yan, Chang Zhou, and  
584 Jingren Zhou. Qwen-audio: Advancing universal audio understanding via unified large-scale  
585 audio-language models. *arXiv preprint arXiv:2311.07919*, 2023.
- 586  
587 Konstantinos Drossos, Samuel Lipping, and Tuomas Virtanen. Clotho: An audio captioning dataset.  
588 In *ICASSP 2020-2020 IEEE International Conference on Acoustics, Speech and Signal Processing  
589 (ICASSP)*, pp. 736–740. IEEE, 2020.
- 590  
591 Eduardo Fonseca, Xavier Favory, Jordi Pons, Frederic Font, and Xavier Serra. Fsd50k: an open  
592 dataset of human-labeled sound events. *IEEE/ACM Transactions on Audio, Speech, and Language  
593 Processing*, 30:829–852, 2021.
- 594  
595 Chaoyou Fu, Yuhan Dai, Yondong Luo, Lei Li, Shuhuai Ren, Renrui Zhang, Zihan Wang, Chenyu  
596 Zhou, Yunhang Shen, Mengdan Zhang, et al. Video-mme: The first-ever comprehensive evaluation  
597 benchmark of multi-modal llms in video analysis. *arXiv preprint arXiv:2405.21075*, 2024.
- 598  
599 Jiyang Gao, Chen Sun, Zhenheng Yang, and Ram Nevatia. Tall: Temporal activity localization via  
600 language query. In *Proceedings of the IEEE international conference on computer vision*, pp.  
601 5267–5275, 2017.

- 594 Tiantian Geng, Teng Wang, Jinming Duan, Runmin Cong, and Feng Zheng. Dense-localizing audio-  
595 visual events in untrimmed videos: A large-scale benchmark and baseline. In *Proceedings of the*  
596 *IEEE/CVF Conference on Computer Vision and Pattern Recognition*, pp. 22942–22951, 2023.  
597
- 598 Rohit Girdhar, Alaaeldin El-Nouby, Zhuang Liu, Mannat Singh, Kalyan Vasudev Alwala, Armand  
599 Joulin, and Ishan Misra. Imagebind: One embedding space to bind them all. In *Proceedings of the*  
600 *IEEE/CVF Conference on Computer Vision and Pattern Recognition*, pp. 15180–15190, 2023.  
601
- 602 Arushi Goel, Zhifeng Kong, Rafael Valle, and Bryan Catanzaro. Audio dialogues: Dialogues dataset  
603 for audio and music understanding. *arXiv preprint arXiv:2404.07616*, 2024.
- 604 Yuan Gong, Hongyin Luo, Alexander H Liu, Leonid Karlinsky, and James Glass. Listen, think, and  
605 understand. *arXiv preprint arXiv:2305.10790*, 2023.  
606
- 607 Shawn Hershey, Daniel PW Ellis, Eduardo Fonseca, Aren Jansen, Caroline Liu, R Channing Moore,  
608 and Manoj Plakal. The benefit of temporally-strong labels in audio event classification. In *ICASSP*  
609 *2021-2021 IEEE International Conference on Acoustics, Speech and Signal Processing (ICASSP)*,  
610 pp. 366–370. IEEE, 2021.
- 611 De-An Huang, Shijia Liao, Subhashree Radhakrishnan, Hongxu Yin, Pavlo Molchanov, Zhiding  
612 Yu, and Jan Kautz. Lita: Language instructed temporal-localization assistant. *arXiv preprint*  
613 *arXiv:2403.19046*, 2024.
- 614 Sahar Kazemzadeh, Vicente Ordonez, Mark Matten, and Tamara Berg. Referitgame: Referring to  
615 objects in photographs of natural scenes. In *Proceedings of the 2014 conference on empirical*  
616 *methods in natural language processing (EMNLP)*, pp. 787–798, 2014.  
617
- 618 Chris Dongjoo Kim, Byeongchang Kim, Hyunmin Lee, and Gunhee Kim. Audiocaps: Generating  
619 captions for audios in the wild. In *Proceedings of the 2019 Conference of the North American*  
620 *Chapter of the Association for Computational Linguistics: Human Language Technologies, Volume*  
621 *1 (Long and Short Papers)*, pp. 119–132, 2019.
- 622 Zhifeng Kong, Arushi Goel, Rohan Badlani, Wei Ping, Rafael Valle, and Bryan Catanzaro. Audio  
623 flamingo: A novel audio language model with few-shot learning and dialogue abilities. *arXiv*  
624 *preprint arXiv:2402.01831*, 2024.  
625
- 626 Ranjay Krishna, Kenji Hata, Frederic Ren, Li Fei-Fei, and Juan Carlos Niebles. Dense-captioning  
627 events in videos. In *Proceedings of the IEEE international conference on computer vision*, pp.  
628 706–715, 2017.
- 629 Guangyao Li, Yake Wei, Yapeng Tian, Chenliang Xu, Ji-Rong Wen, and Di Hu. Learning to answer  
630 questions in dynamic audio-visual scenarios. In *Proceedings of the IEEE/CVF Conference on*  
631 *Computer Vision and Pattern Recognition*, pp. 19108–19118, 2022.  
632
- 633 Junnan Li, Dongxu Li, Silvio Savarese, and Steven Hoi. Blip-2: Bootstrapping language-image  
634 pre-training with frozen image encoders and large language models. In *International conference*  
635 *on machine learning*, pp. 19730–19742. PMLR, 2023a.
- 636 KunChang Li, Yanan He, Yi Wang, Yizhuo Li, Wenhai Wang, Ping Luo, Yali Wang, Limin Wang, and  
637 Yu Qiao. Videochat: Chat-centric video understanding. *arXiv preprint arXiv:2305.06355*, 2023b.  
638
- 639 Zhaowei Li, Qi Xu, Dong Zhang, Hang Song, Yiqing Cai, Qi Qi, Ran Zhou, Junting Pan, Zefeng Li,  
640 Vu Tu, et al. Groundinggpt: Language enhanced multi-modal grounding model. In *Proceedings*  
641 *of the 62nd Annual Meeting of the Association for Computational Linguistics (Volume 1: Long*  
642 *Papers)*, pp. 6657–6678, 2024.
- 643 Samuel Lipping, Parthasaarathy Sudarsanam, Konstantinos Drossos, and Tuomas Virtanen. Clotho-  
644 aqa: A crowdsourced dataset for audio question answering. In *2022 30th European Signal*  
645 *Processing Conference (EUSIPCO)*, pp. 1140–1144. IEEE, 2022.  
646
- 647 Haotian Liu, Chunyuan Li, Qingyang Wu, and Yong Jae Lee. Visual instruction tuning. *Advances in*  
*neural information processing systems*, 36, 2024.

- 648 Ruipu Luo, Ziwang Zhao, Min Yang, Junwei Dong, Da Li, Pengcheng Lu, Tao Wang, Linmei Hu,  
649 Minghui Qiu, and Zhongyu Wei. Valley: Video assistant with large language model enhanced  
650 ability. *arXiv preprint arXiv:2306.07207*, 2023.
- 651  
652 Chenyang Lyu, Minghao Wu, Longyue Wang, Xinting Huang, Bingshuai Liu, Zefeng Du, Shuming  
653 Shi, and Zhaopeng Tu. Macaw-llm: Multi-modal language modeling with image, audio, video,  
654 and text integration. *arXiv preprint arXiv:2306.09093*, 2023.
- 655 Muhammad Maaz, Hanoona Rasheed, Salman Khan, and Fahad Shahbaz Khan. Video-chatgpt:  
656 Towards detailed video understanding via large vision and language models. *arXiv preprint*  
657 *arXiv:2306.05424*, 2023.
- 658 Kathleen McKeown. *Text generation*. Cambridge University Press, 1992.
- 659  
660 Xinhao Mei, Chutong Meng, Haohe Liu, Qiuqiang Kong, Tom Ko, Chengqi Zhao, Mark D Plumbley,  
661 Yuexian Zou, and Wenwu Wang. Wavcaps: A chatgpt-assisted weakly-labelled audio captioning  
662 dataset for audio-language multimodal research. *IEEE/ACM Transactions on Audio, Speech, and*  
663 *Language Processing*, 2024.
- 664 Andreea-Maria Oncescu, Joao F Henriques, Yang Liu, Andrew Zisserman, and Samuel Albanie.  
665 Query: A video dataset with high-quality text and audio narrations. In *ICASSP 2021-2021 IEEE*  
666 *International Conference on Acoustics, Speech and Signal Processing (ICASSP)*, pp. 2265–2269.  
667 IEEE, 2021.
- 668  
669 Karol J Piczak. Esc: Dataset for environmental sound classification. In *Proceedings of the 23rd ACM*  
670 *international conference on Multimedia*, pp. 1015–1018, 2015.
- 671 Alec Radford, Jong Wook Kim, Chris Hallacy, Aditya Ramesh, Gabriel Goh, Sandhini Agarwal,  
672 Girish Sastry, Amanda Askell, Pamela Mishkin, Jack Clark, et al. Learning transferable visual  
673 models from natural language supervision. In *International conference on machine learning*, pp.  
674 8748–8763. PMLR, 2021.
- 675 Muhammad Mamunur Rashid, Guiqing Li, and Chengrui Du. Nonspeech7k dataset: Classification  
676 and analysis of human non-speech sound. *IET Signal Processing*, 17(6):e12233, 2023.
- 677  
678 Jeff Rasley, Samyam Rajbhandari, Olatunji Ruwase, and Yuxiong He. Deepspeed: System optimiza-  
679 tions enable training deep learning models with over 100 billion parameters. In *Proceedings of*  
680 *the 26th ACM SIGKDD International Conference on Knowledge Discovery & Data Mining*, pp.  
681 3505–3506, 2020.
- 682 Shuhuai Ren, Linli Yao, Shicheng Li, Xu Sun, and Lu Hou. Timechat: A time-sensitive multimodal  
683 large language model for long video understanding. In *Proceedings of the IEEE/CVF Conference*  
684 *on Computer Vision and Pattern Recognition*, pp. 14313–14323, 2024.
- 685  
686 Justin Salamon, Christopher Jacoby, and Juan Pablo Bello. A dataset and taxonomy for urban sound  
687 research. In *Proceedings of the 22nd ACM international conference on Multimedia*, pp. 1041–1044,  
688 2014.
- 689 Fangxun Shu, Lei Zhang, Hao Jiang, and Cihang Xie. Audio-visual llm for video understanding.  
690 *arXiv preprint arXiv:2312.06720*, 2023.
- 691  
692 Jianlin Su, Murtadha Ahmed, Yu Lu, Shengfeng Pan, Wen Bo, and Yunfeng Liu. Roformer: Enhanced  
693 transformer with rotary position embedding. *Neurocomputing*, 568:127063, 2024.
- 694 Yixuan Su, Tian Lan, Huayang Li, Jialu Xu, Yan Wang, and Deng Cai. Pandagpt: One model to  
695 instruction-follow them all. *arXiv preprint arXiv:2305.16355*, 2023.
- 696  
697 Yansong Tang, Dajun Ding, Yongming Rao, Yu Zheng, Danyang Zhang, Lili Zhao, Jiwen Lu, and Jie  
698 Zhou. Coin: A large-scale dataset for comprehensive instructional video analysis. In *Proceedings*  
699 *of the IEEE/CVF Conference on Computer Vision and Pattern Recognition*, pp. 1207–1216, 2019.
- 700 Yunlong Tang, Daiki Shimada, Jing Bi, and Chenliang Xu. Avicuna: Audio-visual llm with  
701 interleaver and context-boundary alignment for temporal referential dialogue. *arXiv preprint*  
*arXiv:2403.16276*, 2024.

- 702 Hugo Touvron, Thibaut Lavril, Gautier Izacard, Xavier Martinet, Marie-Anne Lachaux, Timothée  
703 Lacroix, Baptiste Rozière, Naman Goyal, Eric Hambro, Faisal Azhar, et al. Llama: Open and  
704 efficient foundation language models. *arXiv preprint arXiv:2302.13971*, 2023.
- 705  
706 A Vaswani. Attention is all you need. *Advances in Neural Information Processing Systems*, 2017.
- 707 Xin Wang, Jiawei Wu, Junkun Chen, Lei Li, Yuan-Fang Wang, and William Yang Wang. VateX: A  
708 large-scale, high-quality multilingual dataset for video-and-language research. In *Proceedings of*  
709 *the IEEE/CVF international conference on computer vision*, pp. 4581–4591, 2019.
- 710  
711 Yi Wang, Yanan He, Yizhuo Li, Kunchang Li, Jiashuo Yu, Xin Ma, Xinhao Li, Guo Chen, Xinyuan  
712 Chen, Yaohui Wang, et al. Internvid: A large-scale video-text dataset for multimodal understanding  
713 and generation. *arXiv preprint arXiv:2307.06942*, 2023.
- 714 Junbin Xiao, Xindi Shang, Angela Yao, and Tat-Seng Chua. Next-qa: Next phase of question-  
715 answering to explaining temporal actions. In *Proceedings of the IEEE/CVF conference on computer*  
716 *vision and pattern recognition*, pp. 9777–9786, 2021.
- 717  
718 Jun Xu, Tao Mei, Ting Yao, and Yong Rui. Msr-vtt: A large video description dataset for bridging  
719 video and language. In *Proceedings of the IEEE conference on computer vision and pattern*  
720 *recognition*, pp. 5288–5296, 2016.
- 721 Antoine Yang, Antoine Miech, Josef Sivic, Ivan Laptev, and Cordelia Schmid. Learning to answer  
722 visual questions from web videos. *arXiv preprint arXiv:2205.05019*, 2022a.
- 723  
724 Pinci Yang, Xin Wang, Xuguang Duan, Hong Chen, Runze Hou, Cong Jin, and Wenwu Zhu. Avqa:  
725 A dataset for audio-visual question answering on videos. In *Proceedings of the 30th ACM*  
726 *international conference on multimedia*, pp. 3480–3491, 2022b.
- 727 Zhou Yu, Dejing Xu, Jun Yu, Ting Yu, Zhou Zhao, Yueting Zhuang, and Dacheng Tao. Activitynet-qa:  
728 A dataset for understanding complex web videos via question answering. In *Proceedings of the*  
729 *AAAI Conference on Artificial Intelligence*, volume 33, pp. 9127–9134, 2019.
- 730  
731 Abhay Zala, Jaemin Cho, Satwik Kottur, Xilun Chen, Barlas Oguz, Yashar Mehdad, and Mohit  
732 Bansal. Hierarchical video-moment retrieval and step-captioning. In *Proceedings of the IEEE/CVF*  
733 *Conference on Computer Vision and Pattern Recognition*, pp. 23056–23065, 2023.
- 734 Hang Zhang, Xin Li, and Lidong Bing. Video-llama: An instruction-tuned audio-visual language  
735 model for video understanding. *arXiv preprint arXiv:2306.02858*, 2023.
- 736  
737 Luowei Zhou, Chenliang Xu, and Jason Corso. Towards automatic learning of procedures from web  
738 instructional videos. In *Proceedings of the AAAI Conference on Artificial Intelligence*, volume 32,  
739 2018.
- 740  
741  
742  
743  
744  
745  
746  
747  
748  
749  
750  
751  
752  
753  
754  
755

756 APPENDIX

757  
758 A DEMO PAGE LINK

759 The link to our demo page is <https://om-cat.github.io/>.

760  
761  
762 B ALGORITHM FOR ROTARY TIME EMBEDDINGS (RoTE)

763 Below, we present the algorithm for applying RoTE to the visual feature embeddings,  $h_v$ . The same  
764 algorithm applies to audio features,  $h_a$ .

---

765 **Algorithm 1** Rotary Time Embeddings (RoTE)

---

766 *Require:*  $h_{v_x}$ : List of  $x$ -coordinates for visual features,  $h_{v_y}$ : List of  $y$ -coordinates for visual features,  
767  $\tau$ : timestamp for the video frames,  $d$ : Embedding dimension,  $N$ : number of video frames

768 *Ensure:* Rotated coordinates  $(h_{v_{x_{rot}}}, h_{v_{y_{rot}}})$

769 1:  $freqs \leftarrow \text{linspace}(0, 1, d/2)$   $\triangleright$  Frequency adjustments based on dimension

770 2: **for**  $i = 1$  to  $N$  **do**

771 3:  $\theta \leftarrow -\tau_i \times 2\pi$   $\triangleright$  Angle for rotation

772 4:  $rot\_angle \leftarrow \theta \times freqs[-1]$   $\triangleright$  Rotation using the highest frequency

773 5:  $h_{v_{x_{rot}}}[i] \leftarrow h_{v_x}[i] \times \cos(rot\_angle) - h_{v_y}[i] \times \sin(rot\_angle)$

774 6:  $h_{v_{y_{rot}}}[i] \leftarrow h_{v_x}[i] \times \sin(rot\_angle) + h_{v_y}[i] \times \cos(rot\_angle)$

775 7: **end for**

776 8: **return**  $(h_{v_{x_{rot}}}, h_{v_{y_{rot}}})$

---

780  
781 C PROMPTS FOR GENERATING OCTAV DATASET

782 In this section, we discuss further details about generating our proposed dataset.

783  
784 C.1 PROMPTS FOR OCTAV-ST DATASET

785 Below we show the prompts used to generate question-answer pairs for the video conditioned on a  
786 single audio event *i.e.* OCTAV-ST dataset.

787  
788  
789  
790  
791  
792  
793  
794  
795  
796  
797  
798  
799  
800  
801  
802  
803  
804  
805  
806  
807  
808  
809

810  
811  
812  
813  
814  
815  
816  
817  
818  
819  
820  
821  
822  
823  
824  
825  
826  
827  
828  
829  
830  
831  
832  
833  
834  
835  
836  
837  
838  
839  
840  
841  
842  
843  
844  
845  
846  
847  
848  
849  
850  
851  
852  
853  
854  
855  
856  
857  
858  
859  
860  
861  
862  
863

You are an AI assistant that can analyze a video. You receive timestamped video and audio captions with start time and end times describing the video you are observing. Based on these audio and video captions, create 2 question and answer pairs where a question is asked by the person (the user) and the answer is given by you (the assistant) about the events in the video/audio. Here are some additional requirements about the generated question-answer pairs:

1. The question asked by the user should be from the audio caption and the answer given by the assistant should be from the video caption before or after that timestamp in question.
  2. Only describe what you are certain about, and avoid providing descriptions that maybe ambiguous or inaccurate.
  4. The number of words in the answer should not exceed 100 words. Keep it as concise as possible. You do not need to include everything in the answer.
- Include timestamp information in the answers.

Example 1:

Timestamped video and audio captions:

“video caption 1”: season the chicken on both sides with salt and pepper then cut it into pieces from 0.0 to 18, “video caption 2”: put the chicken pieces to a boiling pot of water cover it and let it cook from 20 to 22, “audio caption”: There is a sound of Trumpet from 18 to 20.

QA:

User: What is happening in the video before the sound of trumpet? Assistant: The sound of trumpet is from [18.0, 20.0]. From [0.0, 18.0], the chicken is seasoned on both sides with salt and pepper then cut it into pieces.

User: What is happening in the video after the sound of trumpet? Assistant: The sound of trumpet is from [18.0, 20.0]. From [20.0, 22.0], the chicken pieces are put to a boiling pot of water, covered and then cooked.

Based on the example above, design 2 question and answer pairs between the user and assistant for the example given below.

Format each QA pair in a single line as a JSON dictionary (key “user” for question, and “assistant” for answer).

## C.2 PROMPTS FOR OCTAV-MT DATASET

Below we show the prompts used to generate question-answer pairs for the video conditioned on two audio events *i.e.* OCTAV-MT dataset.



864 You are an AI assistant that can analyze a video. You receive timestamped video and audio  
 865 captions with start time and end times describing the video you are observing. Based on these  
 866 audio and video captions, create 4 question and answer pairs where a question is asked by the  
 867 person (the user) and the answer is given by you (the assistant) about the events in the video/audio.  
 868 You can ask clarification questions if the question asked by the user is not clear. Here are some  
 869 additional requirements about the generated question-answer pairs:  
 870 1. The question asked by the user can be from the audio caption or the video caption and the  
 871 answer given by the assistant should be from the video caption before or after that timestamp in  
 872 question.  
 873 2. Only describe what you are certain about, and avoid providing descriptions that maybe  
 874 ambiguous or inaccurate.  
 875 4. The number of words in the answer should not exceed 100 words. Keep it as concise as possible.  
 876 You do not need to include everything in the answer.  
 877 Include timestamp information in the answers.  
 878  
 879 Example 1:  
 880 Timestamped video and audio captions:  
 881 “video caption 1”: season the chicken on both sides with salt and pepper then cut it into pieces  
 882 from 0.0 to 18, “video caption 2”: put the chicken pieces to a boiling pot of water cover it and let  
 883 it cook from 20 to 22, “video caption 3”: chop celery to small pieces chop cheese to cubes and  
 884 chop ham also to the same size from 26 to 50, “audio caption 1”: There is a sound of laugh from  
 885 18 to 20, “audio caption 2”: There is a sound of laugh from 22 to 26.  
 886 QA:  
 887 User: What is happening in the video after the sound of laugh? Answer with start and end  
 888 timestamps.  
 889 Assistant: There are two sounds of laugh, one from [18.0, 20.0] and the other one from [22.0,  
 890 26.0]. Which laugh are you referring to?  
 891 User: I am referring to the laugh that happens after the chicken pieces are out to a boiling pot of  
 892 water.  
 893 Assistant: Okay, so the laugh from [22.0, 26.0]. After this sound of laugh from [26.0, 50.0], celery  
 894 is chopped to small pieces, cheese is chopped to cubes and ham is chopped also to the same size.  
 895 User: Thanks, what is happening in the video after the chicken is seasoned on both sides with salt  
 896 and pepper. Answer with start and end timestamps.  
 897 Assistant: There is a sound of laugh from [18.0, 20.0] and from [20.0, 22.0], the chicken pieces  
 898 are put ot a boiling pot of water, covered and cooked.  
 899 User: Thanks, what is happening in the video after the sound of bird chirping? Answer with start  
 900 and end timestamps.  
 901 Assistant: Sorry, there is no sound of bird chirping.  
 902  
 903 Based on the above examples, design 4 question and answer pairs between the user and assistant  
 904 for the example given below.  
 905 Format each QA pair in a single line as a JSON dictionary (key “user” for question, and “assistant”  
 906 for answer, wrapped with and ).

### 907 C.3 LIST OF INSTRUCTIONS

909 Below, we show the diverse set of instructions that we use to replace the common instruction *What*  
 910 *is happening in the video* generated by the GPT model. The *eventname* below is replaced by the  
 911 anchored query such as *after the sound of bird chirping*.  
 912  
 913  
 914  
 915  
 916  
 917

918  
919  
920  
921  
922  
923  
924  
925  
926  
927  
928  
929  
930  
931  
932  
933  
934  
935  
936  
937  
938  
939  
940  
941  
942  
943  
944  
945  
946  
947  
948  
949  
950  
951  
952  
953  
954  
955  
956  
957  
958  
959  
960  
961  
962  
963  
964  
965  
966  
967  
968  
969  
970  
971

Start and end timestamps should be included while describing what *eventname* is.

Please include the start and end time when briefly describing what *eventname* entails.

Start and end timestamps are required while providing a brief description of what *eventname* involves.

Include the exact start and end times when describing what *eventname* refers to.

Ensure to mention the start and end timestamps when explaining what *eventname* covers.

With the start and end times, please provide a brief explanation of what *eventname* is.

Start and end timestamps should be given alongside a description of what *eventname* involves.

When describing what *eventname* is, include the exact start and end time information.

Include start and end time details when summarizing what *eventname* entails.

Start and end timestamps must be specified when giving a brief description of what *eventname* refers to.

Describe what *eventname* is with start and end timestamps.

Please briefly describe what *eventname* entails, including its exact start and end timestamps.

Provide a brief description of what *eventname* includes, along with the start and end times.

Give a short description of what *eventname* is, including the precise start and end time details.

Briefly explain what *eventname* involves, including its start and end timestamps.

Please summarize what *eventname* covers, specifying the start and end timestamps.

Give a brief explanation of what *eventname* is, making sure to include both the start and end times.

Could you describe what *eventname* refers to, including the exact start and end times?

Please provide a concise overview of what *eventname* involves, along with start and end time details.

Could you explain what *eventname* is, ensuring the start and end timestamps are included?

#### C.4 SOUND EVENTS

In this section, we provide details about the datasets we used for adding sound to the curated chunked videos as discussed in Section 3. Specifically, we use Urban Sound 8K (Salamon et al., 2014), ESC-50 (Piczak, 2015), FSD50K (Fonseca et al., 2021) and NonSpeech7K (Rashid et al., 2023) datasets.

Urban Sound 8K (Salamon et al., 2014) is an audio dataset that contains urban sounds from 10 classes: air conditioner, car horn, children playing, dog bark, drilling, engine idling, gun shot, jackhammer, siren, and street music.

The ESC-50 dataset (Piczak, 2015) consists of 5-second-long recordings organized into 50 semantical classes that can be categorized into 5 major categories of animals, natural soundscapes & water sounds, human and non-speech sounds, interior/domestic sounds and exterior/urban noises.

972 FSD50K (Fonseca et al., 2021) has 200 sound categories mainly produced by physical sound sources  
973 and production mechanisms, including human sounds, sounds of things, animals, natural sounds,  
974 musical instruments and more.

975 Nonspeech7k (Rashid et al., 2023) contains a diverse set of human non-speech sounds, such as the  
976 sounds of breathing, coughing, crying, laughing, screaming, sneezing, and yawning.  
977

## 978 D EXAMPLES FROM THE OCTAV DATASET 979

980 In Figure 4, we show examples from the OCTAV-ST dataset. The top part of the figure shows an  
981 example from the ActivityNet subset and the bottom part shows an example from the Youcook2 subset  
982 of the dataset. These examples give an overview of how different event transitions are interwoven  
983 seamlessly with an audio event.  
984

985 In Figure 5 and Figure 6, we show examples from the ActivityNet subset and the Youcook2 subset  
986 of the OCTAV-MT dataset respectively. These examples show the anchoring of transitioning video  
987 events on multiple sound events.

988 In Figure 7, we show an example from the UnAV-100-MT dataset, which is the multi-turn version  
989 of the UnAV-100 dataset (Geng et al., 2023). We convert the audio-visual timestamped annotations  
990 from the UnAV-100 dataset into multi-turn question answers as shown in this example. This dataset  
991 acts as a benchmark for a real time setting of audio-visual scenarios.  
992

993  
994  
995  
996  
997  
998  
999  
1000  
1001  
1002  
1003  
1004  
1005  
1006  
1007  
1008  
1009  
1010  
1011  
1012  
1013  
1014  
1015  
1016  
1017  
1018  
1019  
1020  
1021  
1022  
1023  
1024  
1025

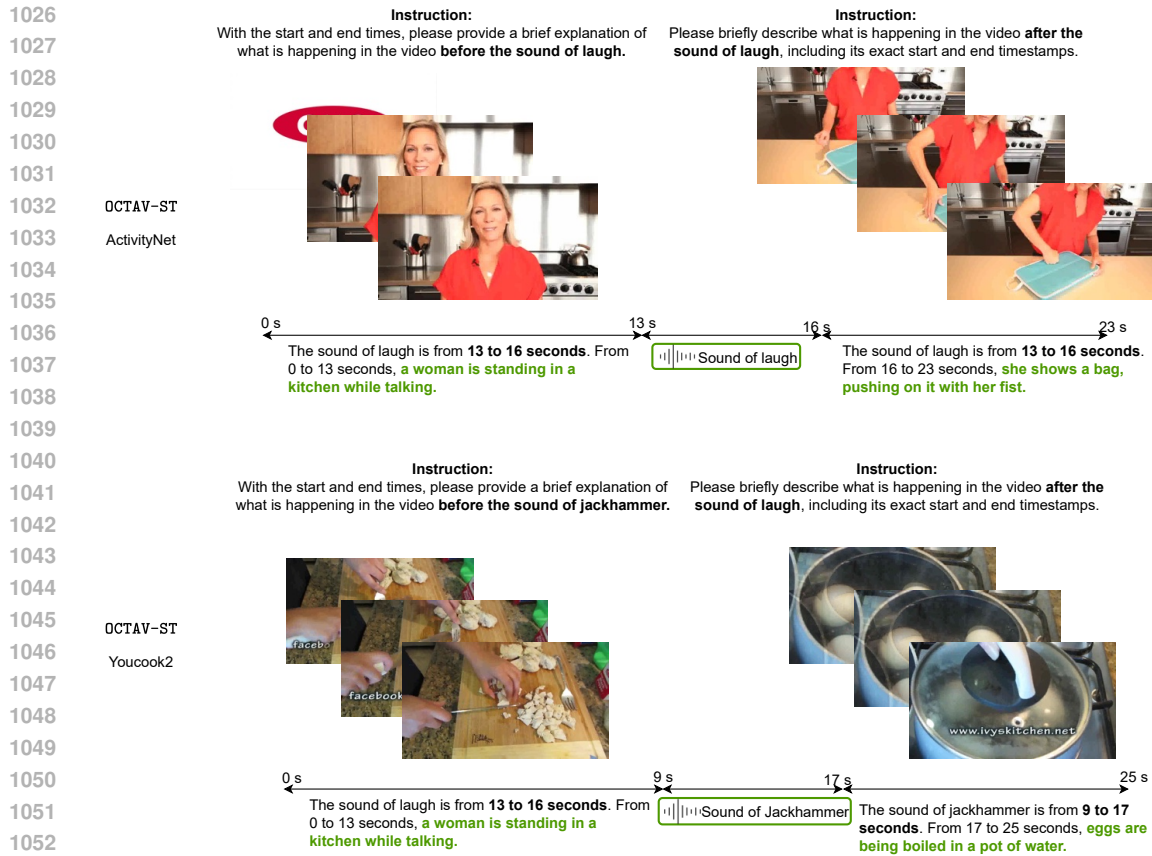


Figure 4: Question-answer pairs from the proposed OCTAV-ST dataset.

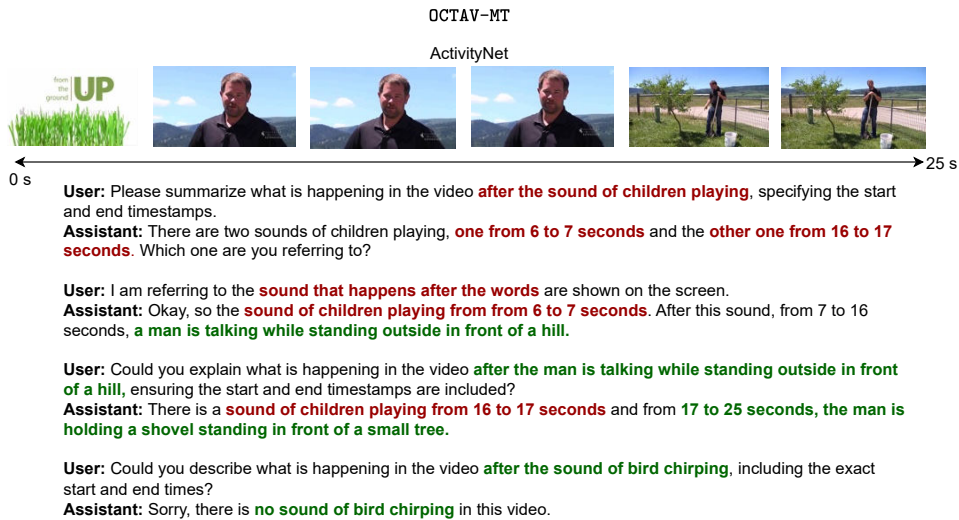


Figure 5: Multi-turn dialogue examples from the ActivityNet subset of our OCTAV-MT dataset.

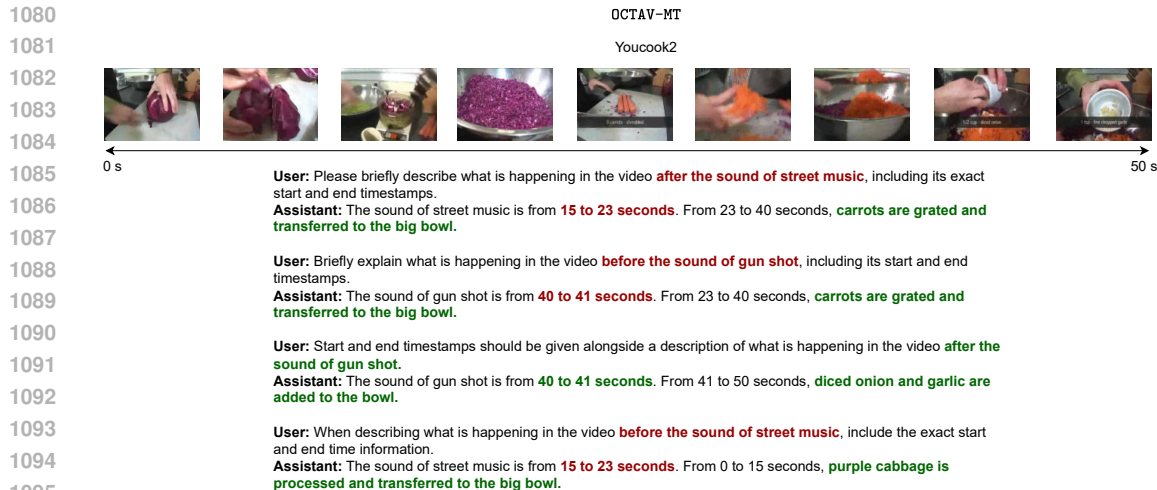


Figure 6: Multi-turn dialogue examples from the Youcook2 subset of our OCTAV-MT dataset.

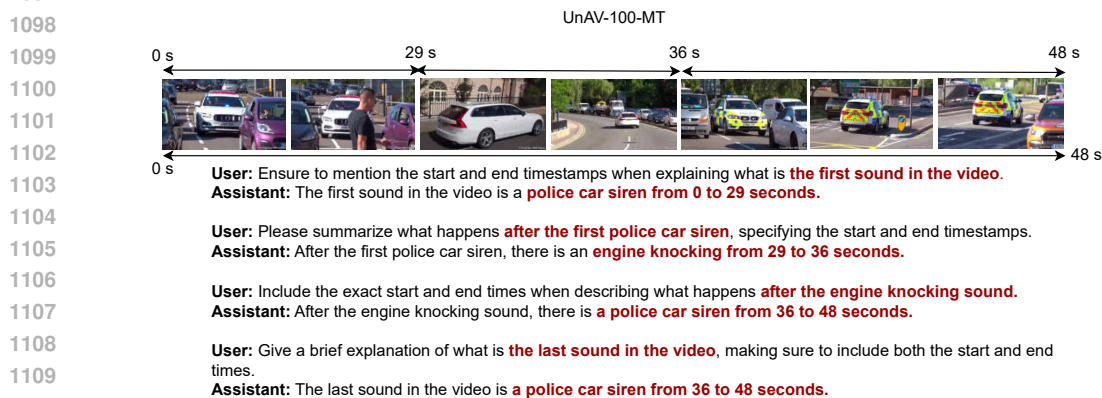


Figure 7: Multi-turn dialogue examples from the UnAV-100-MT dataset.

## 1114 E TRAINING DETAILS

1115 The training settings for our model are spread across three stages, each with specific configurations.

1116 Stage 1 utilizes a batch size of 64 and a learning rate of  $1e-3$ , employing a cosine decay learning schedule. The warm-up ratio is set at 0.03, with no weight decay applied. This stage runs for 1 epoch with gradient accumulation of 1. Additionally, it employs the ZeRO2 optimization strategy in DeepSpeed (Rasley et al., 2020) and utilizes 8 A100 GPUs.

1121 Stage 2 has a smaller batch size of 32 and reduces the learning rate to  $2e-5$ . It follows the same warm-up ratio of 0.03 and applies no weight decay. Like Stage 1, this stage runs for 1 epoch but increases gradient accumulation to 2. The same DeepSpeed optimization and GPU configuration are used.

1126 Stage 3 mirrors the settings of Stage 2, with a batch size of 32, a learning rate of  $2e-5$ , and a warm-up ratio of 0.03. It also has no weight decay and runs for 1 epoch with gradient accumulation set to 2. We use the same DeepSpeed optimization and 8 A100 GPUs like the previous stages.

## 1130 F MORE RESULTS

1131 In Table 9, we showcase the zero-shot performance of our proposed OMCAT model on the video understanding benchmarks MSRVT-QA (Xu et al., 2016), MSVD-QA (Chen & Dolan, 2011), and ActivityNet-QA (Yu et al., 2019). Although our model’s performance falls short compared to Video

LLaMA 2 (Cheng et al., 2024) and AVicuna (Tang et al., 2024), it remains competitive with other models in the field (Li et al., 2024; Zhang et al., 2023; Li et al., 2023b). We attribute AVicuna’s higher performance to its instruction tuning with ActivityNet captions (Krishna et al., 2017) and its specialization in video understanding during the final training stage. Similarly, Video LLaMA 2 (Cheng et al., 2024) is also an expert model, having been trained on a significantly larger video-text dataset throughout all training phases, unlike OMCAT.

We further assess our method’s effectiveness in audio understanding by evaluating it on the Cloth-AQA (Lipping et al., 2022) dataset, where OMCAT achieves a score of 54.3% in audio question answering. In comparison, the audio expert model Qwen-Audio (Chu et al., 2023) scores 57.9%, while Video LLaMA 2 reaches 59.7%. Our model demonstrates competitive performance on this benchmark; however, we believe that the extensive audio-text training data utilized by these two models contributes to their superior results. Moreover, we use Imagebind (Girdhar et al., 2023) as our audio encoder whereas these models use a far more superior audio encoder pre-trained on a large-scale audio-text data unlike Imagebind (Girdhar et al., 2023). It is worth noting that this aspect was beyond the scope of our work, which primarily focuses on temporal and cross-modal understanding of audio and video.

Table 9: Performance comparison on video understanding benchmarks. † means specialized model and \* means trained on a much larger dataset.

Method	Modality	MSRVTT-QA	MSVD-QA	ActivityNet-QA
VideoChat (Li et al., 2023b)	Video	45.0	56.3	26.5
Video-ChatGPT (Maaz et al., 2023)	Video	49.3	64.9	35.2
Valley (Luo et al., 2023)	Video	45.7	65.4	42.9
Video-LLaMA (Zhang et al., 2023)	Video	29.6	51.6	12.4
PandaGPT (Su et al., 2023)	Video, Audio	23.7	46.7	11.2
MacawLLM (Lyu et al., 2023)	Video, Audio	25.5	42.1	14.5
AVLLM (Shu et al., 2023)	Video, Audio	53.7	67.3	47.2
GroundingGPT (Li et al., 2024)	Video, Audio	51.6	67.8	44.7
AVicuna† (Tang et al., 2024)	Video, Audio	<b>59.7</b>	70.2	<b>53.0</b>
Video LLaMA 2* (Cheng et al., 2024)	Video, Audio	53.9	<b>71.7</b>	49.9
OMCAT (RoPE (Su et al., 2024))	Video, Audio	49.3	63.2	41.9
OMCAT (ITT)	Video, Audio	51.1	65.1	43.9
OMCAT (RoTE)	Video, Audio	51.2	67.8	46.6

## G LIMITATIONS AND FUTURE WORK

Here, we outline some limitations that are important considerations for future work.

First, the OCTAV dataset consists of sounds that are non-overlapping and distinct, which simplifies the learning and classification process. However, in real-life scenarios, sound events often overlap, occur simultaneously, and can be highly ambiguous. This makes sound detection and classification far more complex. Thus, a natural extension of our work would be to incorporate sound data that reflects more in-the-wild conditions, where sounds are less controlled, overlap frequently, and can exhibit high variability in intensity and duration. Adapting the dataset to represent such real-world complexities will enhance the robustness and applicability of the model in practical applications.

Second, our proposed OMCAT model employs the CLIP visual encoder (Radford et al., 2021) as the video encoder, which focuses on frame-based visual representations. While CLIP has demonstrated strong capabilities in multimodal learning, it lacks explicit modeling of temporal dynamics between video frames. Given that many real-world events are temporally dependent—especially in video sequences—using a video-based encoder that captures temporal consistency, such as those designed for action recognition (Ren et al., 2024), would likely result in more accurate and nuanced representations of events. In future work, we aim to explore alternative video encoders that model temporal aspects of video more effectively, enabling better alignment between the visual and audio modalities in complex, dynamic environments. This could lead to more sophisticated models capable of handling temporal dependencies and multi-event interactions in both visual and audio data.

Third, currently the dataset consists of short-length videos (~30-40 seconds), extending the dataset to long videos would be extremely beneficial for practical applications. Longer videos would provide more comprehensive context, allowing models to better capture temporal dependencies, complex patterns, and interactions that unfold over extended periods. Moreover, long-duration videos would

1188 enable more robust testing and evaluation in real-world scenarios, where short clips often fail to  
1189 represent the full dynamics of real-time events. Expanding the dataset in this way would lead to more  
1190 accurate models and improve their generalizability across a broader range of applications.  
1191

1192

1193

1194

1195

1196

1197

1198

1199

1200

1201

1202

1203

1204

1205

1206

1207

1208

1209

1210

1211

1212

1213

1214

1215

1216

1217

1218

1219

1220

1221

1222

1223

1224

1225

1226

1227

1228

1229

1230

1231

1232

1233

1234

1235

1236

1237

1238

1239

1240

1241